AMP complex becomes of zero net charge and the NMR spectrum becomes broad, suggesting long stacks.

There is a significant contrast between the equimolar $enPd^{2+}$ complexes of AMP and those of IMP or GMP. The $(enPd^{2+}AMP^{2-})^0$ complex at pH 6 contains a dinegative phosphate group. Addition of a proton to yield a uninegative phosphate at pH 3.5 yields shorter stacks, the NMR spectrum of which appears in Figure 1. The NMR spectrum in Figure 2 corresponds at pH 8 to short stacks of $(edPd^{2+}IMP^{3-})^-$, which contains in addition to a dinegative phosphate a negative charge on the nucleic base due to deprotonation at N(1). The complex of net zero charge appears at pH 5 and is produced by adding a proton mainly to the phosphate group. This addition makes it of a single negative charge while there also remains a negative charge on the nucleic base. Thus the charge distribution differs in the two overall neutral complexes of $enPd^{2+}$. The AMP^{2-} complex at pH 6 contains a dinegative phosphate while the IMP^{2-} complex at pH 5 contains a uninegative phosphate and a negatively charged purine base.

In reference to the introduction section, not one item of information garnered in this research demands or even suggests the presence of N(7)–O(6) chelation in oxopurines or N(7)–N(6) chelation in adenine derivatives. On the contrary, this investigation has confirmed once again that a deprotonated N(1) site in a purine is a metal binding site. With two or more coordination positions available on a metal ion, the availability of both N(7) and N(1) purine sites leads easily to polymer formation, which is extensive in complexes of net zero charge.

Acknowledgment. We are grateful to Dr. Per Ivar Vestues for discussions concerning this research.

Note Added in Proof. Recent work by Dr. P. I. Vestues in this laboratory indicates significant hypochromic effects in ultraviolet absorption spectra and enhanced circular dichroism magnitudes in solutions where polymer formation is proposed in this paper.

Registry No. AMP, 61-19-8; IMP, 131-99-7; Pd, 7440-05-3.

Contribution from the Dipartimento di Chimica, Università di Perugia, 06100 Perugia, Italy

Metal–Metal Interactions in One Dimension. 2.[1] Electronic Structure of Palladium(II) Dithioacetates

G. CIULLO and O. PIOVESANA*

Received July 16, 1979

The electronic structures of the monomeric $Pd(CH_3CSS)_2$ and dimeric $Pd_2(CH_3CSS)_4$ molecules have been investigated by using an approximate, parameter-free LCAO–MO–SCF method. The total energy of PdL_2 is found to be almost exactly half that of Pd_2L_4, in agreement with the coexistence of the two molecules in solution. Calculated excitation energies are in good agreement with experimental optical data. The Pd–Pd interactions in the dimer are of bonding type and are interpreted as mainly due to the metal $4d_{z^2}$ and $5p_z$ orbitals. The possible role of intermolecular Pd–Pd interactions in determining the one-dimensional solid-state arrangements of PdL_2 and Pd_2L_4 is discussed.

Introduction

The highly anisotropic properties of one-dimensional inorganic systems are assumed in general to be due to one-dimensional d_{z^2} bands lying at the Fermi level.[2] This implies, in general, structures built up by planar molecules stacking, as closely as possible, along the normal to their planes.[2] A point of crucial importance in the design of such new materials, and which is still matter of controversy, is whether the M–M interactions can be responsible for the adoption of the desired columnar structure or whether the structure is favored by lattice energy considerations and its natural adoption permits these interactions. The general problem is to ascertain the extent to which the electronic structures of the repeat units can determine the observed crystal structures. E.g., recent theoretical work has shown that the $Pt(CN)_4^{2-}$ chains[3] of $K_2Pt(CN)_4(H_2O)_3$ and the metal chains of the Magnus green salt[4] are antibonding and essentially nonbonding, respectively. The main reason appears to be that, contrary to previous assumptions, the mainly d_{z^2} orbitals on the isolated units of these compounds lie well below[4,5] the highest occupied energy level, and appreciable solid-state interactions and/or partial oxidation must occur in order to have bound states and to raise the d_{z^2} band up to the Fermi level.[3,4]

In the preceding paper[1] we described the preparation, constitution, and structure of the dithioacetic acid derivatives of palladium(II). The X-ray structures of two phases, based on a common 2:1 ligand to metal ratio, involve linear chains of directly interacting metal atoms, with short M–M contacts, as a result of a one-dimensional arrangement of either dimeric (structure B) or alternating monomeric and dimeric units[6] (structure A), i.e.

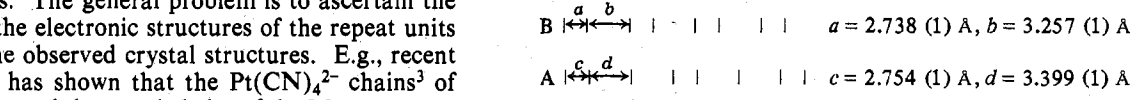

These structural patterns are of interest in light of the empirical fact that the vast majority of the d^8 complexes involving 1,1- or 1,2-dithiolato ligands adopt essentially monomeric, often laterally displaced structures which do not allow short M–M contacts.[7] It is of further interest that the rather unique

(1) Part 1: Piovesana, O.; Bellitto, C.; Flamini, A.; Zanazzi, P. F. *Inorg. Chem.* **1979**, *18*, 2258.
(2) For reviews see: Miller, J. S.; Epstein, A. J. *Prog. Inorg. Chem.* **1976**, *20*, 1. Krogmann, K. *Angew. Chem., Int. Ed. Engl.* **1969**, *8*, 35. Thomas, T. W.; Underhill, A. E. *Chem. Soc. Rev.* **1972**, *1*, 99.
(3) Whangbo, M. H.; Hoffmann, R. *J. Am. Chem. Soc.* **1978**, *100*, 6093.
(4) Interrante, L. V.; Messmer, R. P. *Inorg. Chem.* **1971**, *10*, 1174.
(5) Interrante, L. V.; Messmer, R. P. *Chem. Phys. Lett.* **1974**, *26*, 225; *Adv. Chem. Ser.* **1975**, *No. 5*, 382.
(6) The monomeric molecule has been assumed to be planar (the maximum deviation from the least-squares plane is 0.02 Å). The dimer involves four bridging ligands. The distance between the S_4 planes is 0.14 Å longer than the Pd–Pd distance. The two parallel S_4 squares are rotated in a tetragonal twist from the eclipsed D_{4h} structure by 22.5° in form A and 25° in form B. Other structural parameters are in ref 1.
(7) Eisenberg, R. *Prog. Inorg. Chem.* **1970**, *12*, 295. Holm, R. H.; O'Connor, M. J. *Ibid.* **1971**, *14*, 306.

0020-1669/80/1319-2871$01.00/0

Table I. Interatomic Distances (Å) and Angles (Deg) Used in the Calculations[a,b]

	Pd-S	S-C	C-C	Pd-Pd	SPdS	SCS	PdSC
monomer	2.331	1.680	1.470		73.7	112.7	86.8
dimer	2.326	1.676	1.515	2.738	90.0	128.8	109.8

[a] See also footnote 6. [b] The structural parameters of the dimer refer to structure B.

presence of both the PdL_2 and Pd_2L_4 molecules in structure A, with different bonding within the chelated rings and different spectra, is not due to solid-state effects since the two molecules coexist also in solution and in the gas phase.[1]

This paper reports a theoretical investigation of the electronic structures of the monomeric and dimeric molecules. A main aim is to achieve a quantitative understanding of the Pd to Pd bonding in the dimer and also to consider possible relationships between the electronic structures of the isolated PdL_2 and Pd_2L_4 units and the different M–M interactions, as indicated by the X-ray data, along the metal chains of the A and B structures. The two molecules are still too complex to be treated extensively by rigorous methods. We have used an approximate, parameter-free LCAO–MO–SCF method,[8] which was successfully applied to the analysis of the electronic structures of several dithio complexes of Ni(II). This method involved an extensive use of the Mulliken-type approximations and a point charge approximation to the whole of the two-center interactions experienced by a given orbital charge distribution. Two modifications of this procedure have been examined here: (i) the use of theoretical instead of empirical one-center integrals in the calculation of the SCF matrix elements; (ii) the substitution of the Mulliken approximation with that of Löwdin,[9] both in the population analysis and in the calculation of the SCF matrix elements. The Löwdin approximation is computationally more demanding but theoretically more accurate since it preserves, besides the total charge, the dipole moment.

Computational Details

In both the Löwdin and Mulliken approximations, the $\chi_a\chi_b$ charge distribution is shared between the χ_a and χ_b orbitals according to

$$\chi_a\chi_b = \lambda_a\chi_a\chi_a + \lambda_b\chi_b\chi_b$$

where $\lambda_a + \lambda_b = S_{ab}$. Rotational invariance with respect to the local axes is ensured if λ_a transforms like S_{ab}. In the Mulliken approximation this occurs because $\lambda_a = {}^1/_2 S_{ab}$. In the Löwdin approximation, λ_a is a more complex function of S_{ab}, and, to make it rotationally invariant, we used the procedure[10] in which the quantity in question is calculated with reference to a conventional axis set (with σ and π characters with respect to the internuclear axis) and then transformed to the required axis set in the same way as S_{ab}. Care has been taken to calculate the molecular interactions with the same approximations used in the calculation of the SCF matrix elements.[11] Some details are reported in the Appendix, together with a description of the calculation of the core repulsion.

Average values (Table I) of interatomic distances and angles[1] have been used to ensure C_{2v} and D_2 symmetries to the PdL_2 and Pd_2L_4 molecules,[6] respectively, by an appropriate location of the hydrogen atoms. The geometry of the methyl group was that optimized in the staggered conformation of ethane.[12] Due to the presence of the hydrogen atoms, the sulfur atoms in the dimer split up into two symmetry nonequivalent (S and S′) sets. The hydrogen atoms form two distinct sets in the monomer and three (H′, H″, and H‴) in the dimer. An obvious distinction is made between nonmethylic and methylic carbon atoms (C′ and C″, respectively).

In both PdL_2 and Pd_2L_4 the local z axes are perpendicular to the S_4 planes. In PdL_2 the Pd y axis passes through the carbon atoms. In Pd_2L_4 the Pd x and y axes point to the carbon atoms when translated, along the z axis, to the midpoint of the Pd–Pd distance. The σ characters of the carbon and sulfur orbitals are defined with respect to the C–C and S–Pd bonds, respectively. The π_h and π_v labels of the same orbitals refer to the planes of the chelating CS_2 groups. The σ, π_h, and π_v characters have an approximate significance in the dimer, since the z axes, which are parallel to the Pd–Pd line, are defined of π_h symmetry. The largest atomic basis set included the palladium 4d, 5s, and 5p, the carbon 2s and 2p, the sulfur 3s, 3p, and 3d, and the hydrogen 1s valence orbitals. The SCF functions of Gray et al.[13] have been used for palladium. The s and p functions of carbon and sulfur were those of Clementi for the ^3P state.[14] The sulfur 3d orbitals were Slater-type functions with an exponent of 1.5, a value optimized in ab initio calculations.[15] The hydrogen atom was represented by a 1s Slater function with an exponent of 1.2. In the empirical calculations, the one-center integral values of Oleari et al.,[16] with reference states +1 for palladium and 0 for the other atoms, were employed.

Results and Discussion

Population Analysis and One-Center Integrals. Table II lists the various calculations carried out, together with the resulting atomic charges, total energies, and lowest energy electronic transitions.

The results of calculations 2 and 4 show that the effect of substituting the Löwdin for the Mulliken approximation is substantial. This in itself points out that the Löwdin procedure, which is more rigorous, has to be preferred. More reliable atomic charges and transition energies were obtained in calculation 4 than in calculation 1, i.e., by using theoretical instead of empirical one-center integrals. E.g., the C″ atomic charge is +0.987 in calculation 4 and −3.382 in calculation 1. The anomalous charge distribution in calculation 1 is probably caused by the nonconsistency between the values of the empirical one-center integrals and those of the theoretical two-center interactions. Since one- and two-center integrals are difficult to correlate,[17] a uniform use of theoretical integrals is preferable. Although this removes any electron correlation correction, it better balances the computational parameters. The Löwdin approximation and theoretical one-center integrals were, therefore, used in all the remaining calculations.

The Monomeric Molecule. The relevant highest occupied and lowest virtual MO's of PdL_2 and Pd_2L_4, according to calculations 4 and 5, respectively, are reported in Table III. The total overlap populations, according to the same calculations, are in Table IV.

The ground state of PdL_2 is $...(8b_2)^2(5a_2)^2(6b_1)^2(9a_1)^2 = {}^1A_1$. The interactions of the metal orbitals with the ligands do not follow a crystal field scheme. There is an efficient mixing of metal and ligand orbitals, and, further, distinct sequences of mainly metal MO's are not discernible. Keeping this in mind, the relative ordering of the "d-like" orbitals in

(8) Ciullo, G.; Sgamellotti, A. *Z. Phys. Chem. (Wiesbaden)* **1976**, *100*, 67.
(9) Löwdin, P. O. *J. Chem. Phys.* **1953**, *21*, 374.
(10) Brown, R. D.; Roby, K. R. *Theor. Chim. Acta* **1970**, *16*, 175.
(11) Ciullo, G.; Sgamellotti, A.; Casagrande, F.; Morcellini, M. *Atti Accad. Naz. Lincei, Cl. Sci. Fis. Nat., Rend.* **1975**, [8] *58*, 935.
(12) Stevens, R. M. *J. Chem. Phys.* **1970**, *52*, 1397.
(13) Basch, H.; Gray, H. B. *Theor. Chim. Acta* **1966**, *4*, 367.
(14) Clementi, E. *IBM J. Res. Dev., Suppl.* **1965**, *9*, 2.
(15) Fischer, C. R.; Kemmey, P. J. *Mol. Phys.* **1971**, *22*, 1133.
(16) Tondello, E.; Di Sipio, L.; De Michelis, G.; Oleari, L. *Inorg. Chim. Acta* **1971**, *5*, 305. Oleari, L.; Di Sipio, L.; De Michelis, G. *Mol. Phys.* **1966**, *10*, 97.
(17) Ciullo, G.; Semprini, E.; Sgamellotti, A. *Gazz. Chim. Ital.* **1972**, *102*, 994.

Table II. Some Results of the Calculations[a]

calcn[b]	atomic charges Pd	S	S′	C′	C″	H′	H″	H‴	total energy	transition energies[c]
1, ELBF	1.305	−1.294		2.678	−3.382	0.883	0.878		−18 298	40.3, 41.6, 46.7, 58.2, 60.5, 66.1
2, TMBF	2.266	−1.122		1.274	−1.715	0.526	0.513		−20 201	32.6, 48.1, 52.6, 56.0, 58.7, 60.7
3, TLAF	2.037	−0.834		0.557	0.976	−0.273	−0.298		−20 463	26.3, 29.7, 34.1, 37.1, 41.0, 42.4
4, TLBF	2.104	−0.864		0.559	0.987	−0.277	−0.296		−20 215	33.1, 35.6, 36.4, 36.7, 43.1, 45.1
5, TLBD	1.997	−0.874	−0.879	0.624	0.995	−0.278	−0.298	−0.289	−40 442	46.5, 48.9, 49.0, 49.2, 49.7, 50.3
6, TLCF	1.880	−0.815		0.583	0.958	−0.271	−0.290		−20 154	22.4, 27.6, 28.5, 38.4, 41.0, 43.6
7, TLCD	1.867	−0.838	−0.843	0.628	0.974	−0.275	−0.294	−0.286	−40 368	41.7, 44.4, 46.3, 47.9, 48.4, 48.8

[a] Energies in 10^3 cm^{-1}. [b] T, theoretical one-center integrals; E, empirical one-center integrals; L, Löwdin approximation; M, Mulliken approximation; A, with palladium 5s and 5p and sulfur 3d orbitals; B, with 5s and 5p and without 3d; C, without 5s and 5p and 3d; F, monomer; D, dimer. [c] Lowest allowed electronic transition energies.

Table III. Eigenvalues and Eigenvectors[a]

monomer MO	eigenvalue	eigenvector	dimer MO	eigenvalue	eigenvector
$6a_2$	69.5	1.01f + 0.40k + 0.16i	$18b_1$	134.7	−1.43s + 0.55k + 0.54l + 0.32z + 0.26i + 0.25j + 0.17u
$11a_1$	56.6	1.03z − 0.33p + 0.21v	18a	99.6	1.37s − 0.49k − 0.48l + 0.31z − 0.29t − 0.21c
$9b_2$	7.8	0.99v − 0.69p − 0.27w + 0.21y	17a	58.5	−1.00e + 0.32k − 0.32l + 0.15v + 0.14i − 0.14j
$10a_1$	5.0	−0.97v + 0.64p + 0.26w − 0.20y + 0.16z	$17b_1$	56.2	1.00e − 0.31k + 0.31l − 0.13t − 0.10i + 0.10j
$9a_1$	−71.2	0.87c + 0.49k − 0.17m − 0.12t	$16b_1$	45.7	1.04z − 0.19c − 0.16v + 0.15u − 0.13m − 0.13n
$6b_1$	−73.6	0.93p + 0.45g	16a	27.7	−1.02z − 0.12c
$5a_2$	−76.2	1.00p	$15b_1$	6.3	0.90v + 0.46p + 0.46q − 0.28u + 0.23w − 0.17y + 0.14z
$8b_2$	−82.3	0.89h − 0.41p − 0.22v	14a	−75.5	0.73p + 0.73q + 0.25m + 0.26n
$5b_1$	−87.2	0.70k + 0.62m + 0.34u − 0.14y − 0.12i	$14b_1$	−78.4	0.85c + 0.35k + 0.31l − 0.26m − 0.24n + 0.10s
$4a_2$	−87.9	0.66m + 0.53k + 0.37u − 0.17y − 0.17i	13a	−84.6	0.77c + 0.43k + 0.42l + 0.18t + 0.14r
$4b_1$	−88.7	−0.89g + 0.39p	12a	−86.1	−0.48f − 0.46m + 0.46n + 0.45k − 0.46l + 0.21v + 0.14e
$7b_2$	−92.4	0.82k − 0.42m − 0.36t − 0.35r + 0.12i	$12b_1$	−91.4	0.51p + 0.49q − 0.36v + 0.29m + 0.29n + 0.24c − 0.20w
$8a_1$	−94.0	−0.84p − 0.34v + 0.21w − 0.17y + 0.12z	$10b_1$	−95.1	0.47m + 0.47n + 0.38c − 0.32p − 0.32q − 0.28u
$7a_1$	−94.8	0.95e + 0.28k − 0.20c	11a	−96.4	0.57f − 0.42m + 0.42n + 0.30p − 0.30q + 0.28u + 0.17y
$6a_1$	−99.8	−0.62k + 0.42c + 0.38r + 0.37t + 0.37m	$11b_3$	−97.8	0.77h + 0.54g − 0.25p
			$11b_2$	−97.8	0.76g − 0.56h − 0.25q
			$10b_2$	−48.9	0.67h + 0.46g + 0.41k − 0.22m + 0.15n + 0.15p − 0.15q
			$10b_3$	−98.9	−0.72g + 0.46h − 0.35l + 0.22n − 0.19k + 0.17m − 0.11p
			7a	−106.7	0.59c − 0.44k − 0.44l − 0.31t − 0.26r + 0.13i + 0.13j

[a] Only the most relevant MO's and their principal components, according to calculations 4 and 5, are reported. The following abbreviations are used: $c = 4d_{z^2}$, $e = 4d_{x^2-y^2}$, $f = 4d_{xy}$, $g = 4d_{xz}$, $h = 4d_{yz}$, $i = s(S)$, $j = s(S')$, $k = p_\sigma(S)$, $l = p_\sigma(S')$, $m = p_{\pi_h}(S)$, $n = p_{\pi_h}(S')$, $p = p_{\pi_v}(S)$, $q = p_{\pi_v}(S')$, $r = p_\sigma(C')$, $s = 5s$, $t = p_\sigma(C'')$, $u = p_{\pi_h}(C')$, $v = p_{\pi_v}(C'')$, $z = 5p_z$, $w = s(H')$, $y = s(H'')$. c,e. . . represent symmetry adapted linear combinations of the atomic orbitals of the indicated character, except for g and h in the dimer which represent combinations of $4d_{xz}(Pd_1)$, $4d_{yz}(Pd_2)$ and of $4d_{yz}(Pd_1)$, $4d_{xz}(Pd_2)$, respectively. Eigenvalues are in 10^3 cm^{-1}.

Table IV. Total Overlap Populations[a]

	monomer	dimer
Pd–Pd		0.026
Pd(5s,5p)–S	−0.195 × 4	−0.118 × 4
Pd(5s,5p)–S′		−0.120 × 4
Pd(4d)–S	0.020 × 4	0.009 × 4
Pd(4d)–S′		0.009 × 4
C′–S	0.948 × 4	0.923 × 4
C′–S′		0.920 × 4
C′–C″	0.824 × 2	0.813 × 4
C″–H′	0.767 × 2	0.772 × 4
C″–H″	0.780 × 4	0.791 × 4
C″–H‴		0.777 × 4
total	9.394	19.128

[a] From calculations 4 and 5.

PdL_2 is $4d_{xy} > 4d_{z^2} > 4d_{yz} > 4d_{xz} > 4d_{x^2-y^2}$. d_{z^2} is the main component of the highest occupied MO. The implications of this will be discussed later.

Calculations 3–7 (Table II) place the hydrogen atom at the negative pole of the C–H bond. Although this effect is not expected from the relative electronegativities of carbon and hydrogen, there is agreement that it is present in many molecules.[18] In calculation 4, the 5s and 5p orbitals of palladium are at very high energy. This causes such a small participation in bonding of these orbitals that their population is negative, making the metal charge larger than +2. The effect is due to the theoretical one-center integrals, whose values underestimate the participation of the 5s and 5p to the bonding. With the empirical integrals, calculation 1, the energy difference between the 4d and the 5s, 5p orbitals is, in fact, smaller, and the populations of the latter become positive. In order to keep the effective metal charge apart from the 5s and 5p contributions, we excluded these orbitals from the basis set in calculation 6. A charge of +1.880 was obtained. This value is determined primarily by the σ-donor ability of the chelated ligands, whose π-electron density is mainly localized on the C–S bonds.

Calculations 3 and 4 permit a direct comparison of the effect of introducing the 3d orbitals on sulfur in the basis set. In calculation 3 (with 3d), in spite of the not negligible positive population of 0.039 and 0.010 of the $3d_{x^2-y^2}$ and $3d_{z^2}$ orbitals, respectively, the electronic charge on the sulfur atoms was found to decrease with respect to calculation 4 (without 3d). A similar effect has been inferred in ab initio calculations from the variations of the calculated dipole moment upon inclusion of the 3d orbitals.[19] Such variations result often in disagreement with those of the Mulliken populations.[19,20] The

(18) Daudel, R.; Lefebvre, R.; Moser, C. "Quantum Chemistry-Methods and Applications"; Interscience: New York, 1965; p 205.

(19) Bonaccorsi, R.; Scrocco, E.; Tomasi, J. *J. Chem. Phys.* **1970**, *52*, 5270.
(20) Boer, F. P.; Lipscomb, W. N. *J. Chem. Phys.* **1969**, *50*, 989.

Table V. Spectral Assignment for the Monomer[a]

transitions[b]	transition energies	
	calcd	exptl[d,e]
$9a_1[4d_{z^2},p_\sigma(S)] \rightarrow 6a_2[4d_{xy},3d_{x^2-y^2}(S)]$	24.8[c]	
$9a_1 \rightarrow 10a_1[p\pi_v(C',S)]$	26.3	20.6 (3.47)
$9a_1 \rightarrow 9b_2[p_{\pi_v}(C',S)]$	29.7	22.0 (3.41)
		24.5, 28.6[f]
$8b_2[4d_{yz},p_{\pi_v}(S)] \rightarrow 6a_2$	34.1	34.0 (4.57)
$6b_1[p_{\pi_v}(S), 4d_{xz}] \rightarrow 10a_1$	37.1	37.7 (4.23)
$6b_1 \rightarrow 9b_2$	39.9[c]	
$6b_1 \rightarrow 6a_2$	41.0	40.0 (4.17)
$8a_1[4d_{x^2-y^2},p_\sigma(S)] \rightarrow 6a_2$	41.4[c]	
$5b_1[4d_{xz},p_{\pi_v}(S)] \rightarrow 6a_2$	42.4	43.5 (3.57)
$8b_2 \rightarrow 10a_1$	42.5	

[a] From calculation 3. Energies in 10^3 cm^{-1}. [b] Singlet–singlet, one-electron transitions. The principal components are indicated for each MO. [c] Symmetry forbidden. [d] log ϵ in parentheses. [e] From solution data, see text. Solutions of A in cyclohexane, at room temperature, show absorption maxima (log ϵ in parentheses) at 20.8 (3.04), 22.0 (3.10), ~25 (shoulder), ~26 (shoulder), 30.8 (3.78), 33.9 (4.40), ~35.5 (shoulder), 37.7 (shoulder), 40.5 (4.16), 43.5 (4.10) × 10^3 cm^{-1}. Solutions of B in the same solvent: 25.0 (3.37), 30.8 (3.76), 33.9 (4.27), 35.7 (4.27), 40.8 (4.19), 43.5 (4.23) × 10^3 cm^{-1}. [f] Weak shoulders.

present Löwdin populations reproduce the dipole terms of the electronic distributions, thus pointing out the decrease of the electronic charge on sulfur because of the one-center pd polarization. The main consequence is an increased population of 5s and 5p, hence a smaller metal charge. However, the inclusion of the sulfur 3d orbitals has the most significant influence on the energy levels, and calculation 3, among the five carried out for PdL_2, affords the most reliable energies for the electronic transitions.

Electronic Transitions. The solution behavior of the A and B forms, described in ref 1, allows the energies and intensities of the electronic transitions of PdL_2 to be ascertained. At room temperature, the solution spectrum of the A form can be regarded as resulting from the superposition of the spectra of corresponding quantities of monomers and dimers. Since solutions of the B form contain, at room temperature, dimers only, the molar extinctions of the monomer absorptions (ϵ_M) can be obtained from those of the absorptions of solutions of A (ϵ_A) and B (ϵ_B) through the simple relation: $\epsilon_M = 3\epsilon_A - 2\epsilon_B$, where all the ϵ values are per palladium unit. The energies of the absorption maxima of PdL_2 are confirmed by the variations of the A and B solution spectra which parallel the transformation of Pd_2L_4 into PdL_2 at 80–100 °C.

The assignment of the electronic spectrum of PdL_2, according to calculation 3, is reported in Table V. In agreement with experiment, the calculations predict a series of many closely spaced bands between ~25 000 and ~45 000 cm^{-1}. Making allowance for the approximations involved in the parameter-free method used, the overall agreement between calculated and observed transition energies has to be considered outstanding. According to the assignment in Table V, the band at 20 600 cm^{-1} should be allowed along the z axis (a_1 symmetry in C_{2v}) and that at 22 000 cm^{-1} along the y axis (b_2 symmetry). Preliminary single-crystal polarized spectra of A are in agreement with this prediction and show bands at 20 200 and ~22 000 cm^{-1}, polarized in the stacking direction (z molecular axis, coincident with the crystal a axis) and in the xy molecular plane, respectively. There is, in addition, a broad absorption (z polarized) at ~18 000 cm^{-1}, not present in solutions of either A or B, which can be associated with the one-dimensional character of the crystal lattice. The main change which occurs, in the solution spectra, on going from PdL_2 to Pd_2L_4, is the replacement of the bands at 20 600 and 22 000 cm^{-1} by a single absorption at 25 000 cm^{-1}. In agreement with this pattern, the calculations indicate that the first allowed transition of the dimer, $14b_1 \rightarrow 15a$, still of $4d_{z^2} \rightarrow L_{\pi_v}$ character, occurs at higher energy than the corresponding ones in the monomer, as a consequence of a shift of electron density from C′ to Pd on going from PdL_2 to Pd_2L_4 (vide infra). The remaining transitions of Pd_2L_4 are shifted by the calculations to higher energies, but very much less than the $4d_{z^2} \rightarrow L_{\pi_v}$ transition (Table II). The consequently reduced range of the calculated transition energies and the increased multiplicity (for each transition in the monomer there can be four transitions in the dimer) make the computed transition energies of Pd_2L_4 so close that assignments would be meaningless, expect for that concerning the lowest energy band.

Total Energies. The calculated total energies are in Table II. The values decrease with increasing size of the basis set, as theoretically expected. According to the results of calculations 4 and 5, the total energy of Pd_2L_4 is smaller than twice that of PdL_2 by only 12 000 cm^{-1}. This value, negligible difference between two very large numbers, is in agreement with the observed coexistence of the two molecules in solution and also in the gas phase. As the uncertainty in the energy difference is much greater than kT, the observed behavior is equally attributable to either thermodynamic or kinetic factors.

Bonding in the Dimeric Molecule. The ground state of Pd_2L_4 is $...(14b_3)^2(14b_2)^2(14b_1)^2(14a)^2 = {}^1A$. The results of calculations 4,5 and 6,7 in Table II show that the most significant changes in atomic charge, on going from PdL_2 to Pd_2L_4, occur for the nonmethylic carbon and palladium atoms. More precisely, there is a shift of electron density from C′ to Pd. Actually, if the atomic charges calculated for the monomer are assumed for the dimer, the C′ and Pd atomic levels of Pd_2L_4 are found at higher and lower energy, respectively. The lowering of the palladium charge in the dimer is determined primarily by the 5s and 5p orbitals. As can be seen from Table IV, the negative overlap population (and the consequent negative orbital population) of these empty orbitals decreases considerably as their energy becomes lower. On the other hand, the positive overlap population of the 4d orbitals decreases only slightly on going from the monomer to the dimer. The overall effect is in line with a slightly stronger Pd–S bond in the latter species. The X-ray molecular structures of the two molecules show that a stronger Pd–S bond in the dimer would be favored by the SPdS angle and unfavored by the noncoplanarity of the palladium and sulfur atoms. However, any difference between Pd–S bond lengths is either masked by the inaccuracy of the structural parameters or, perhaps, prevented by steric constraints. The C–C bond length in Pd_2L_4, 1.515 (7) Å, might be larger than in PdL_2, 1.47 (2) Å. If so, this may be traced back to both the higher energy of the C′ atomic levels in Pd_2L_4 (resulting in a smaller overlap population for the C–C, and C–S, bonds) and the larger electrostatic repulsion determined by the higher positive charge of C′ in the dimer. No significant differences can be inferred for the more peripheral C–H bonds.

Besides the short Pd–Pd distance, the "inward" out-of-plane distortion of the palladium atoms in the dimeric structure is indicative of bonding M–M interactions. Accordingly, calculation 5 gives a positive Pd–Pd overlap population of 0.026 electron. The value is mainly due to the 5s, $5p_z$, and $4d_{z^2}$ orbitals, in agreement with the bonding model first suggested by Rundle.[21] This overlap population is likely to underestimate the M–M bond because of the aforementioned underestimate of the 5s and 5p participation. The distance between the S_4 planes, 0.14 Å longer than between the palladium atoms, and the rotation by 25° of the two parallel S_4 planes in a tetragonal twist from the eclipsed D_{4h} structure are understood

(21) Rundle, R. E. *J. Phys. Chem.* **1957**, *61*, 45.

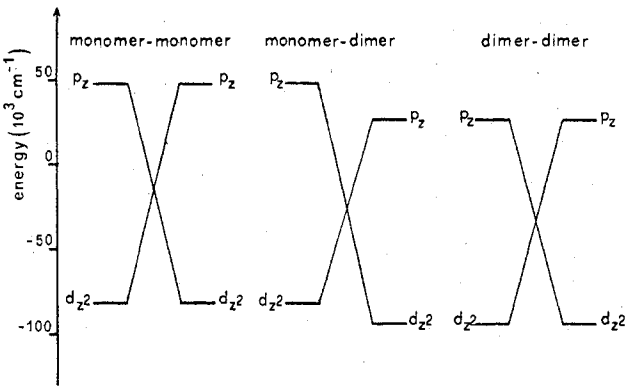

Figure 1. Simplified scheme of the intermolecular Pd–Pd interactions.

as the best compromise between several conflicting drives: the minimization of the repulsion between the negative charges of the sulfur atoms, the coplanarity of sulfurs and palladium, the steric constraint of the ligand (the SCS angle of 128.8° in Pd_2L_4, as compared with that in the free CH_3CSS^- ion, 123.5°,[22] indicates that the chelated ligand is already considerably distorted), and the more favorable energy of a staggered configuration allowing a diamagnetic ground state. A comparison of twice the total overlap population (relative to nearest neighbor atoms) of the monomer, 18.788, with that of the dimer, 19.128, indicates that the overall bonding in PdL_2 is comparable with that in Pd_2L_4, in agreement with the previous total energy considerations.

The M–M Chain. The results of calculations 4 and 5 provide an electronic reason for the different intermolecular metal-repeat separations in the A and B structures.

One simple way to apply the Rundle model to the M–M interaction in Pd_2L_4 is as follows. The filled $4d_{z^2}$ orbital of each palladium combines with the empty $5p_z$ orbital of the other. The effect is a net transfer of charge from $4d_{z^2}$ to $5p_z$ in each palladium. An examination of Table III shows that, for both the monomeric and dimeric molecules, MO's of mainly $5p_z$ character are found among the lowest energy virtual orbitals, and $4d_{z^2}$ mainly contributes to the highest energy filled MO's. Furthermore, at the 3.257 Å interdimer metal-repeat separation in structure B, the overlap between $4d_{z^2}$ and $5p_z$ is calculated as 0.047, a value comparable with that (0.095) calculated at the intradimer Pd–Pd distance of 2.738 Å. These findings seem to indicate that the M–M interactions between adjacent units along the columns are of the same nature as those in a single dimer.

The increased intermolecular metal-repeat separation of 3.399 Å in structure A can be related to the larger energy separation between the mainly $4d_{z^2}$ and mainly $5p_z$ MO's in PdL_2 than in Pd_2L_4. This separation, which is not readily discernible from Table III, because of the multiplicity of the energy levels, may be inferred in a simplified way from the SCF Fock matrix elements of the palladium $4d_{z^2}$ and $5p_z$ orbitals. The energy difference between these orbitals is 129.3 $\times 10^3$ cm^{-1} in PdL_2 and 120.2 $\times 10^3$ cm^{-1} in Pd_2L_4. By using again the $4d_{z^2}$ and $5p_z$ atomic orbitals instead of the related MO's, Figure 1 exemplifies the interactions between different units and suggests more attractive M–M interactions in the following order: monomer–monomer < monomer–dimer < dimer–dimer. Interactions other than interatomic $4d_{z^2}$–$5p_z$ are unlikely to alter the proposed order, which is in agreement with the X-ray data.

As we said before, the columnar structure of the A and B forms are anomalous for d^8 complexes with sulfur ligands. That the $4d_{z^2}$–$5p_z$ interactions may play some role in determining this structural pattern seems to be consistent with the molecular orbital calculations[23] which characterize the d_{z^2} metal orbital as rather lower in energy than the highest occupied levels for sulfur coordinate complexes having no appreciable M–M contacts. The molecular and electronic structures of $Ni(S_2CC_6H_5)_2$, $Ni(S_2CNH_2)_2$, and $Ni(S_2PF_2)_2$ are of interest in this respect. Here it is the $3p_z$ orbital of sulfur to mainly constitute the highest occupied MO's.[8] The $4p_z$-(Ni)–$3p_z$(S) energy separations increase in the order $Ni(S_2CC_6H_5)_2 < Ni(S_2CNH_2)_2 < Ni(S_2PF_2)_2$. In agreement with this, a preferential axial Ni–S interaction seems to be present in the weak lateral trimeric structure of the dithiobenzoato complex (with loose intermolecular Ni–S contacts of ~3.1 Å)[24] and is completely absent in the dithiocarbamato and dithiophosphato complexes, whose structures[25,26] show normal intermolecular contacts and clearly monomeric units.

In conclusion, it appears that electronic factors might play an active role in determining the observed structures, although the packing of the columns in the A and B structures of the palladium dithioacetato system is most likely to be the dominant energy term, as indicated by the instability of the B structure upon elimination of carbon disulfide.[1]

Appendix

$(J_{ij} - aK_{ij})$ contains the Coulomb and exchange interactions between the φ_i and φ_j MO's. $a = 2$ gives the corrections to be subtracted from the differences of eigenvalues in order to have the singlet transition energies. The interelectronic interaction terms in the calculation of the total energy are given by $a = 0.5$. The Coulomb and exchange interactions must be calculated with the same approximations used in the calculation of the SCF matrix elements.[11]

By expanding the MO's as functions of the χ_c atomic orbitals and treating the resultant atomic charge distributions by the method of Löwdin, one gets

$$J_{ij} - aK_{ij} = \sum_{a,b} c_{ai}c_{bi} \sum_{c} n_c(j)\zeta_{ab}^{cc}$$

$n_c(j)$ is the Löwdin electronic population of χ_c resulting from the φ_j MO only. ζ_{ab}^{cc} is the $(J - aK)$ interaction between distribution $\chi_a\chi_b$ and $\chi_c\chi_c$ and is calculated as in the SCF matrix element F_{ab}.[8] The approximations adopted for F_{ab} imply $a = 0.5$ instead of $a = 2$ for the calculation of the transition energies. This, however, is unlikely to be serious, when all the approximations involved are taken into account.

The core repulsion, one of the terms constituting the total energy, has been calculated by providing the cores with a spherical expansion equal to that of the most contracted valence orbital of the atoms.[27] The consequent Coulomb integrals between s functions have been calculated by using a simple approximation,[8] in order not to increase the computational difficulties without substantially improving the results. On the other hand, a calculation of the core repulsion by assuming point cores did not show substantial changes of the total energy patterns.

Registry No. $Pd(CH_3CSS)_2$, 63890-10-8; $Pd(CH_3CSS)_2$ (salt form), 63882-63-3; $Pd_2(CH_3CSS)_4$, 63890-11-9.

(22) Borel, M. M.; Ledesert, M. *Z. Anorg. Allg. Chem.* **1975**, *415*, 285.

(23) Billig, E.; Williams, R.; Bernal, I.; Waters, J. H.; Gray, H. B. *Inorg. Chem.* **1964**, *3*, 663. Davison, A.; Edelstein, N.; Holm, R. H.; Maki, A. H. *Ibid.* **1963**, *2*, 1227. Eisenberg, R.; Ibers, J. A.; Clark, R. J. H.; Gray, H. B. *J. Am. Chem. Soc.* **1964**, *86*, 113. Gray, H. B. *Transition Met. Chem.* **1965**, *1*, 239. Mason, W. R.; Gray, H. B. *J. Am. Chem. Soc.* **1968**, *90*, 5721. Maki, A. H.; Edelstein, N.; Davison, A.; Holm, R. H. *Ibid.* **1964**, *86*, 4580. Shupack, S. I.; Billig, E.; Clark, R. J. H.; Williams, R.; Gray, H. B. *Ibid.* **1964**, *86*, 4594.

(24) Bonamico, M.; Dessy, G.; Fares, V.; Scaramuzza, L. *J. Chem. Soc., Dalton Trans.* **1975**, 2250.

(25) Gasparri, G. F.; Nardelli, M.; Villa, A. *Acta Crystallogr.* **1967**, *23*, 384.

(26) McConnel, J. F.; Kastalsky, V. *Acta Crystallogr.* **1967**, *22*, 853.

(27) Brickstock, A.; Pople, J. A. *Trans. Faraday Soc.* **1954**, *50*, 901. Del Re, G.; Parr, R. G. *Rev. Mod. Phys.* **1963**, *35*, 604.